

Supporting Information

Co₉S₈ decorated into nitrogen/sulfur dual-doped carbon nanofibers as efficient oxygen bifunctional electrocatalyst for Zn–air batteries

Weiwei Zheng, Jiangquan Lv, Huabin Zhang, Hai-Xia Zhang and Jian Zhang*

Experimental Section

Materials: All chemicals were purchased and used without further purification. Cobalt acetate tetrahydrate (Co(CH₃COO)₂·4H₂O, Aladdin Chemistry Co., Ltd., 99%), Sulfur powder (-325 mesh, A Johnson Matthey Company, 99.5%), iridium oxide (IrO₂, Aladdin Industrial Corporation, 99.99%). 20 wt.% Pt/C electrocatalyst (HPT 020) for electrochemical measurements was purchased from Shanghai Hesun Bio.

Synthesis of NC carbon fibers: The polyimide(PI)-based carbon fibers were synthesized by a typical electrospinning method with polyimide as the precursor, followed by annealing process. Firstly, the precursor (PI) was prepared via the polycondensation of 4, 4'-diaminodiphenyl ether(ODA) and 3, 3', 4, 4'-biphenyltetracarboxylic dianhydride (BPDA). A predetermined amount of equimolar ODA and BPDA were dispersed in N, N-dimethylacetamide (DMAc) in a flask, with a solid content of 10 wt.%. Keeping stirring at -3 °C for 24 h, the obtained solution was then loaded in a syringe with a diameter of 0.5 mm spinneret. Electrospinning was performed at a syringe tip to a rotating metal collector (aluminium foil), the distance between the cathode and anode was maintained at 20 cm and a high voltage of 15 kV was applied to the syringe needle tip and the metal collector using a power supply. The typical feeding rate for the coaxial solutions

was set at $0.2 \text{ mL} \cdot \text{h}^{-1}$. Then, the obtained polyimide (PI) -based fiber precursors were aged at a rate of $1 \text{ }^\circ\text{C} \cdot \text{min}^{-1}$ from room temperature to $350 \text{ }^\circ\text{C}$, and kept at this temperature for 2 h in Air. Thereafter, the temperature was heated to $800 \text{ }^\circ\text{C}$ in N_2 at a ramping rate of $5 \text{ }^\circ\text{C} \cdot \text{min}^{-1}$ and kept at this temperature for 4 h to get the NC fibers.

Synthesis of the $\text{Co}_9\text{S}_8/\text{NSC}$ fibers: Typically, 0.06 g of $\text{Co}(\text{CH}_3\text{COO})_2 \cdot 4\text{H}_2\text{O}$ was dissolved into 30 mL of absolute ethyl alcohol under strong ultrasonic. Then, 0.05g of pre-treated polyimide(PI)-based carbon fibers were infiltrated into the prepared solution and kept at $50 \text{ }^\circ\text{C}$ for 5 h. After cooling down, the precursors were dried at room temperature. Finally, the carbon fiber sample (0.05g) and sulfur powder (0.025g) was heated at $800 \text{ }^\circ\text{C}$ for 4 h with a ramping rate of $5 \text{ }^\circ\text{C} \cdot \text{min}^{-1}$ in N_2 . After cooling down to room temperature, Co_9S_8 nanoparticles encapsulated in porous carbon fibers can be achieved, yielding the $\text{Co}_9\text{S}_8/\text{NSC}$ fibers. For comparison, Co/NC nanofibers, NSC and NC nanofibers were also synthesized, respectively.

Characterization : Powder X-ray diffraction (PXRD) analyses were conducted with a MiniFlex II diffractometer with Cu $K\alpha$ radiation ($\lambda = 1.54056 \text{ \AA}$), with a step size of 2. The morphology of the as-prepared catalyst was observed by scanning electron microscopy (SEM, QUANTA FEG 250) and transmission electron microscopy (TEM, JEOL 2100F) inductively coupled high resolution transmission electron microscopy (HRTEM). Energy Dispersive Spectrometer (EDS) tests were carried out with a light element detector via the ZAF technique. The morphology and elemental mapping were performed using Tecnai G2F20. Raman spectroscopy was performed on a LabRAM HR system with an excitation wavelength of 532 nm. X-ray photoelectron spectroscopic (XPS) was performed on ESCALAB 250Xi instrument. N_2

adsorption/desorption measurements (BET, ASAP2020M) were used to identify the specific surface area.

Electrochemical measurements: The electrochemical measurements were carried out at room temperature on an electrochemical workstation (CHI 760E) using a standard three-electrode system. The catalyst coated on glassy carbon rotating disk electrode (diameter 3 mm) was used as a working electrode. A platinum plate and Ag/AgCl electrode (saturated with KCl solution) were employed as the counter and reference electrodes, respectively. All potentials in this study were converted with respect to the reversible hydrogen electrode (RHE) according to the equation ($E_{\text{RHE}} = E_{\text{Ag/AgCl}} + 0.198 + 0.059 \times \text{pH}$). Glassy carbon electrodes were polished before each experiment with 0.05 μm polishing alumina, and ultrasonically cleaned thoroughly with deionized water, ethanol and acetone.

To prepare the working electrode, 5 mg of catalysts and 16 μL of 5 wt% Nafion solutions were dispersed in 1 mL of 1:3 v/v water/isopropanol mixed solvent under sonication to form a homogeneous ink. Subsequently, 2 μL of the catalyst ink was dropped onto the surface of the glass carbon rotating disk electrode and dried at room temperature under air to produce a uniform film with a catalyst loading of 0.15 mg cm^{-2} . The loading of commercial Pt/C was 0.15 mg cm^{-2} .

In ORR experiment, cyclic voltammetry (CV) measurements were carried out in N_2 - or O_2 -saturated 1.0 M KOH solution with a scan rate of 20 mV s^{-1} . Before each experiment, the working electrode was continuously cycled at least 40 times between 0 and 1.0 V (vs. RHE) at a scan rate of 100 mV s^{-1} until a stable CV was recorded. Linear sweep voltammetry (LSV) scans were conducted from 1.1 to 0.2 V (vs. RHE) at a scan rate of 5 mV/s and different rotation speeds (400-2025 rpm) with a rotating disk electrode (RDE). The electron transfer number (n) during

oxygen reduction reaction was calculated at various electrode potential according to the Koutecky-Levich equation,

$$\frac{1}{J} = \frac{1}{J_L} + \frac{1}{J_K} = \frac{1}{B\omega^{1/2}} + \frac{1}{J_K} \quad (1)$$

$$B = 0.62nFC_0(D_0)^{2/3}\nu^{-1/6}$$

(2)

$$J_K = nFKC_0 \quad (3)$$

where J is the measured current density, J_K and J_L are the kinetic- and diffusion-limiting current densities, ω is the angular velocity (rad s^{-1}), n is the transferred electron number per O_2 molecule, F is the Faraday constant ($F = 96485 \text{ C mol}^{-1}$), C_0 is the bulk concentration of O_2 ($1.2 \times 10^{-6} \text{ mol cm}^{-3}$ in 0.1 M KOH electrolyte and $7.8 \times 10^{-7} \text{ mol cm}^{-3}$ in 1.0 M KOH), D_0 is the O_2 diffusion coefficient ($1.9 \times 10^{-5} \text{ cm}^2 \text{ s}^{-1}$ in 0.1 M KOH electrolyte and $1.8 \times 10^{-5} \text{ cm}^2 \text{ s}^{-1}$ in 1.0 M KOH electrolyte), ν is the kinematic viscosity of the electrolyte ($0.01 \text{ cm}^2 \text{ s}^{-1}$) and K is the electron-transfer rate constant.

Electrochemical impedance spectroscopy (EIS) measurement was carried out from 1000 kHz to 100 mHz at the open-circuit voltage of -1.3 V.

For OER experiments, the LSV curves were obtained at a scan rate of 20 mVs^{-1} and in order to obtain a stable current, the LSV data were collected after multiple CV cycles. The electrochemical stability of the sample was performed by chronoamperometric at 0.6 V and 1.7 V.

Zn-air battery measurements: Primary Zn-air batteries were performed in a home-built electrochemical cell. The air cathode was prepared by uniformly dispersing the as-prepared catalyst ink onto teflon-coated carbon fiber paper (1.0 cm^2), then drying it at $60 \text{ }^\circ\text{C}$ for 2 h. The catalyst loading was 0.5 mg cm^{-2} unless otherwise stated. For comparison, Pt/C electrode with

same catalyst loading was also prepared. The polished commercial Zn foil with a thickness of 0.2 mm was used as anode. Both electrodes were constructed into a home-made Zn–air battery in 6 M KOH electrolyte saturated with O₂. All the measurements were conducted on the as-constructed cell at room temperature with CHI 760E electrochemical workstation (Shanghai Chenhua, China).

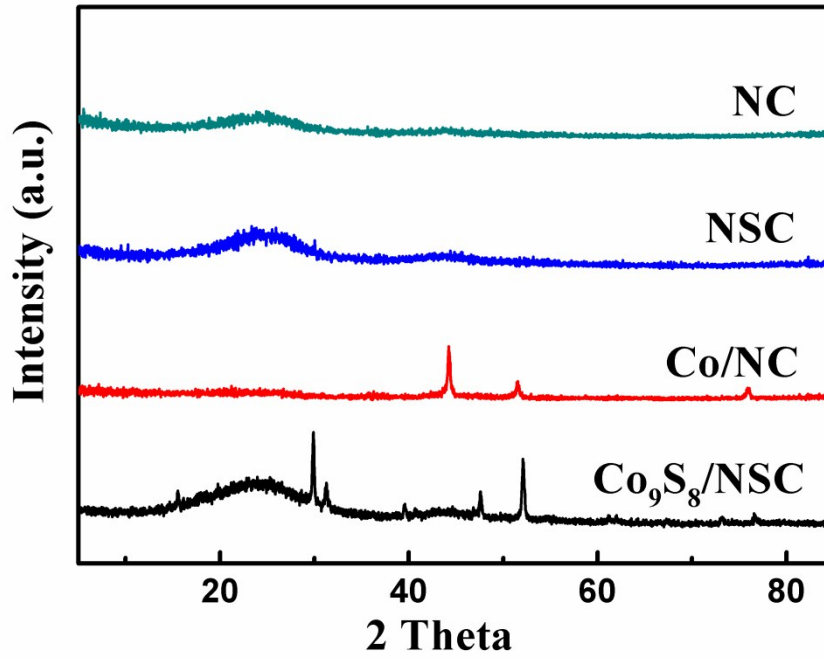


Figure S1. Powder XRD patterns of the $\text{Co}_9\text{S}_8/\text{NSC}$ nanofibers, Co/NC nanofibers, NSC nanofibers, and NC nanofibers.

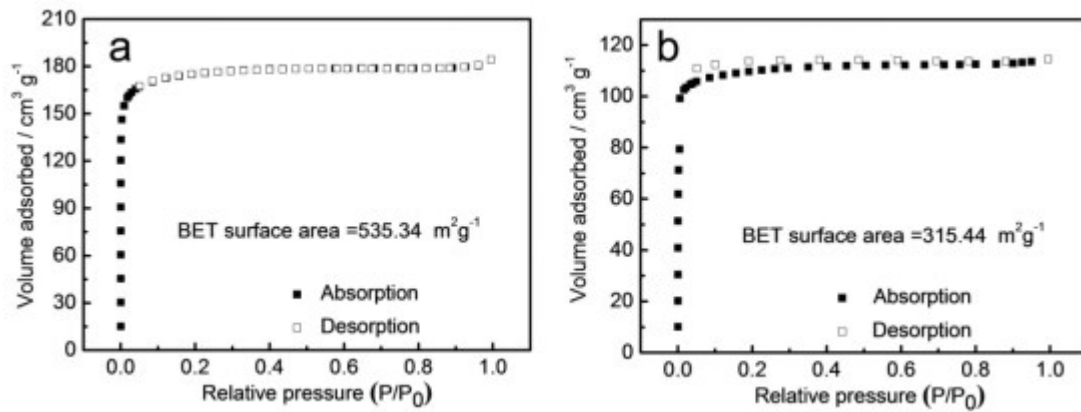


Figure S2. Nitrogen adsorption-desorption isotherm of (a) carbon nanofibers and (b) $\text{Co}_9\text{S}_8/\text{NSC}$ nanofibers.

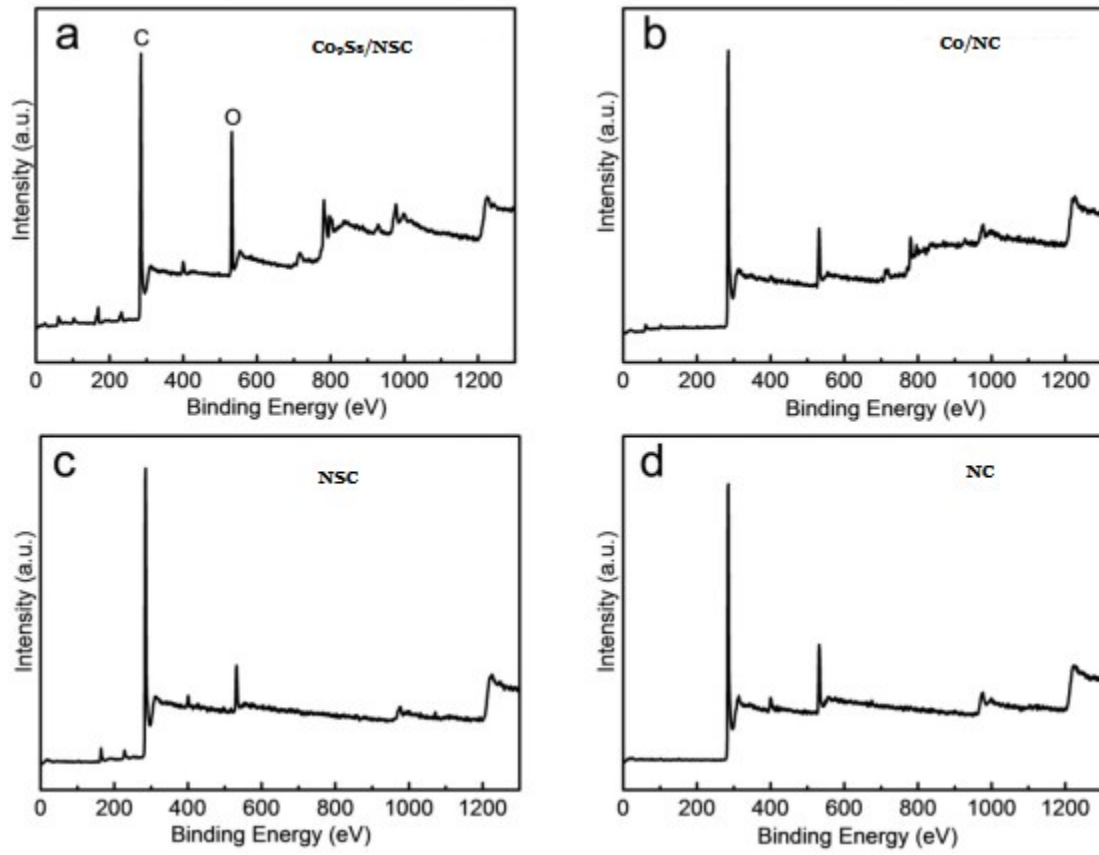


Figure S3. The XPS survey spectrum of the $\text{Co}_9\text{S}_8/\text{NSC}$ nanofibers, Co/NC nanofibers, NSC nanofibers, and NC nanofibers.

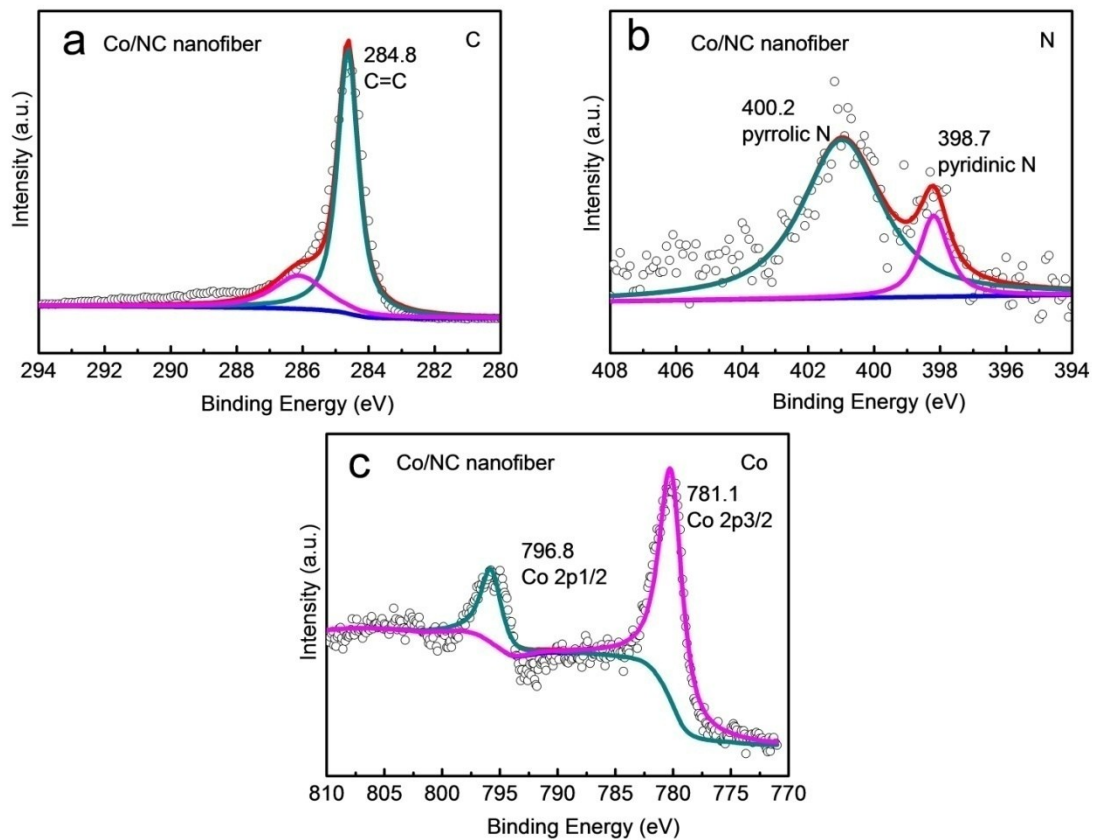


Figure S4. XPS spectra of C 1s; N 1s; Co 2p for the Co/NC nanofibers

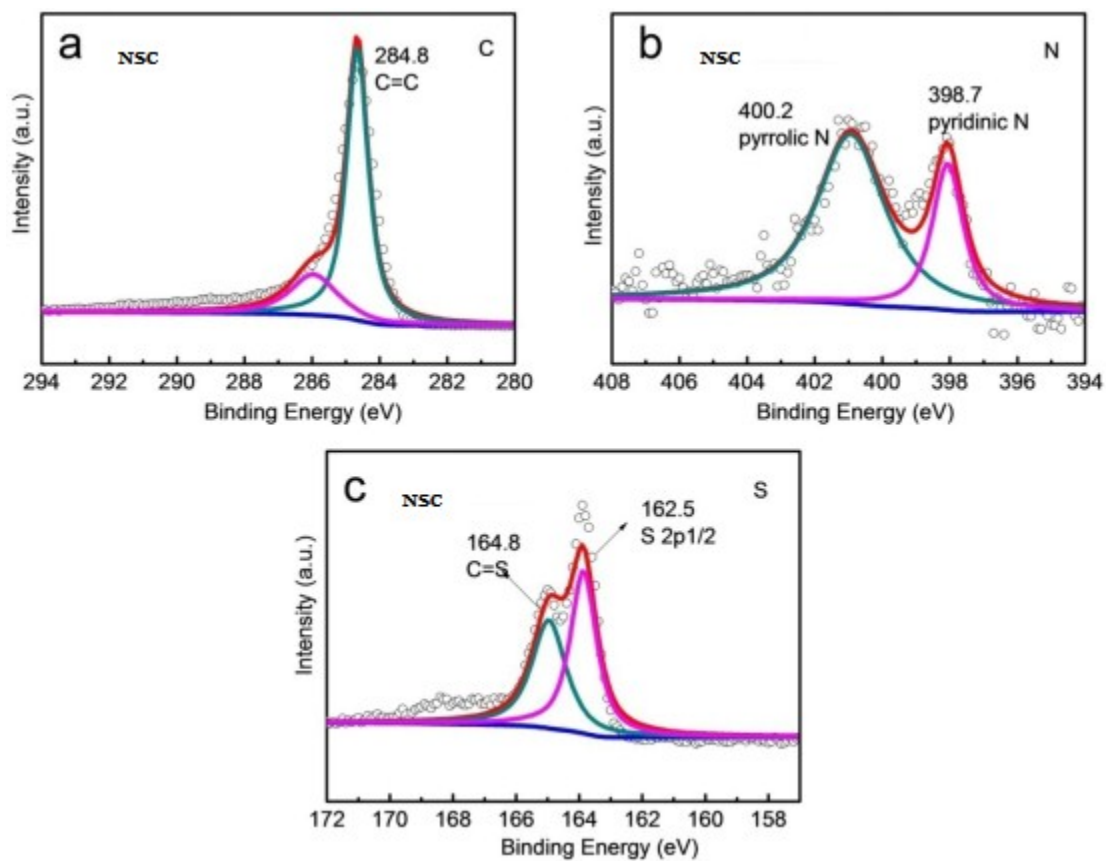


Figure S5. XPS spectra of C 1s; N 1s; S 2p for the NSC nanofibers

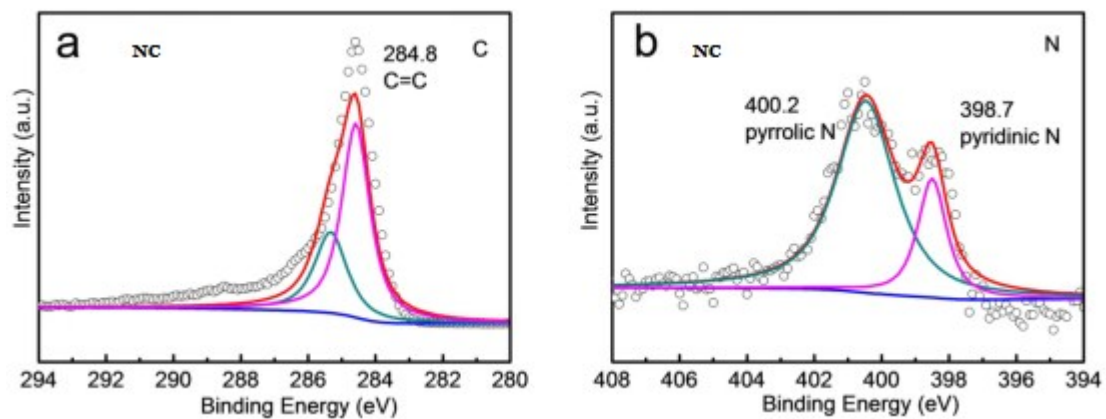


Figure S6. XPS spectra of C 1s; N 1s for the NC nanofibers

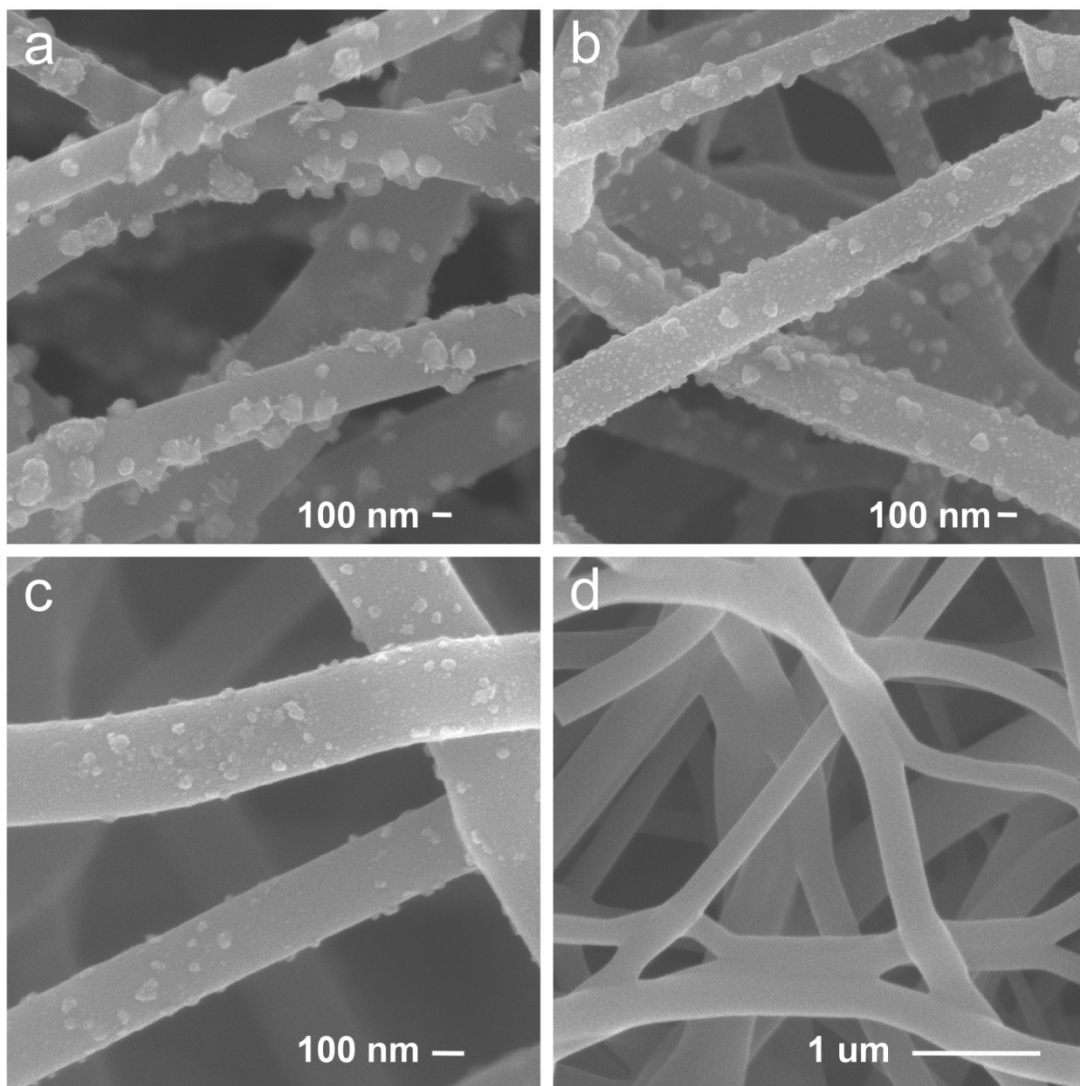


Figure S7. (a-d) SEM images of the $\text{Co}_9\text{S}_8/\text{NSC}$ nanofibers, Co/NC nanofibers, NSC nanofibers, and NC nanofibers.

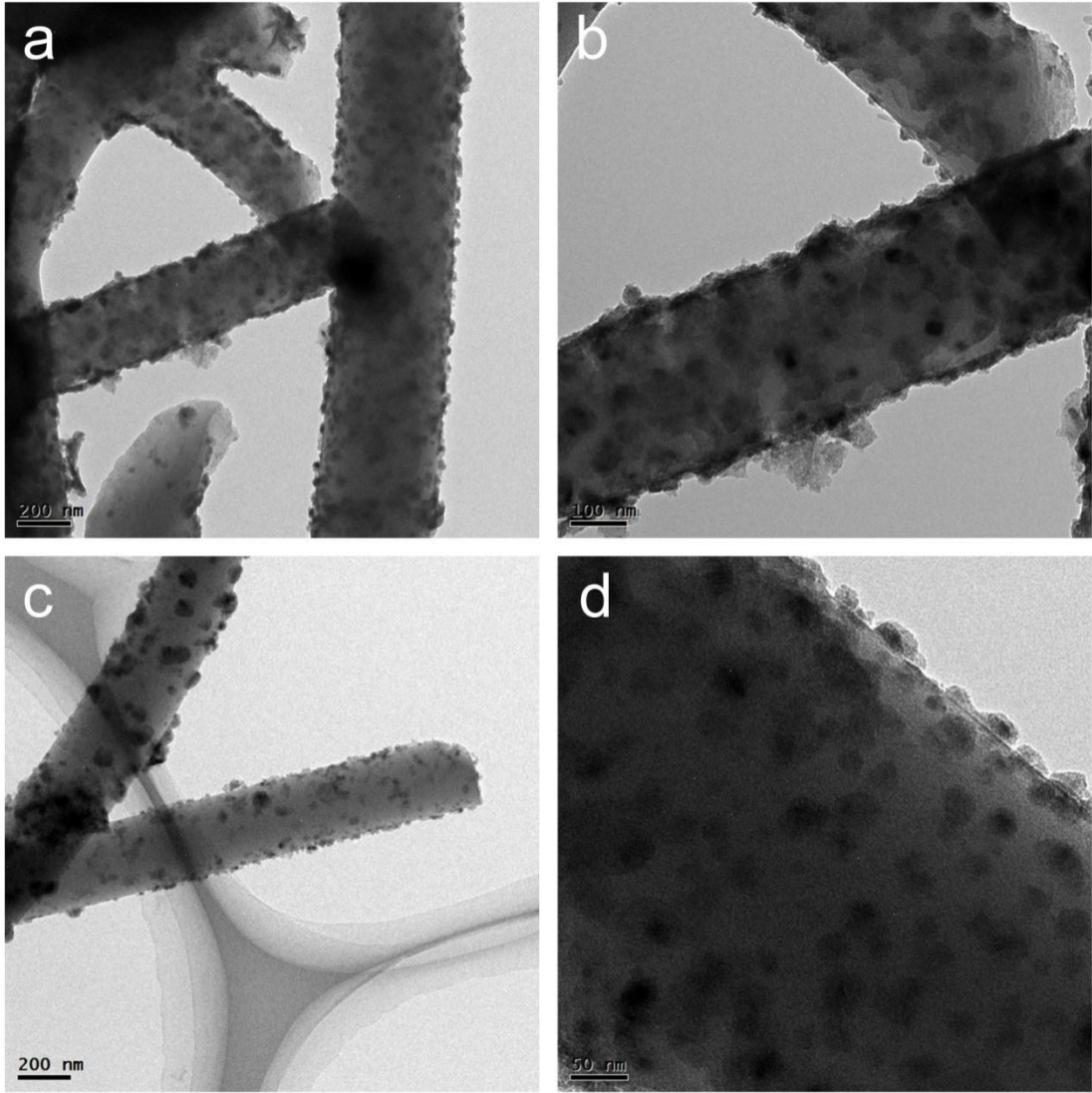


Figure S8. (a-d) TEM images of the Co₉S₈/NSC nanofibers.

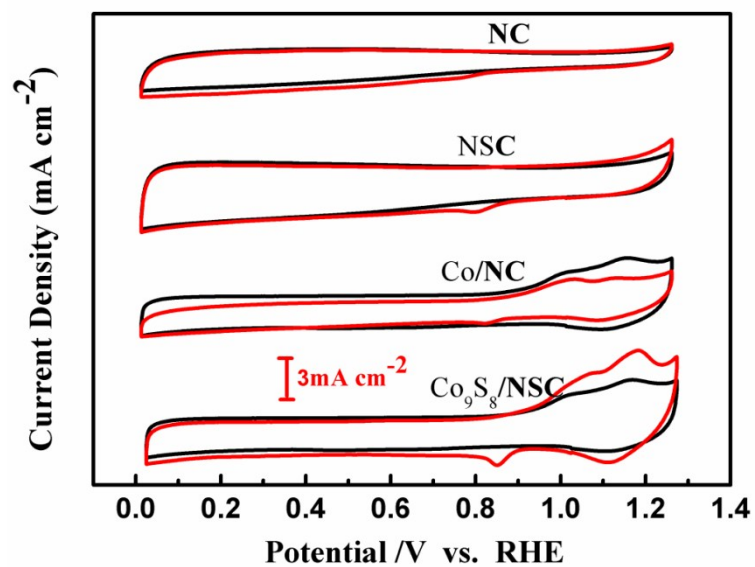


Figure S9. CV curves of the Co₉S₈/NSC nanofibers, Co/NC nanofibers, NSC nanofibers, and NC nanofibers catalysts in (red lines) O₂-and (black lines) N₂-saturated 1 M KOH at 20 mV s⁻¹.

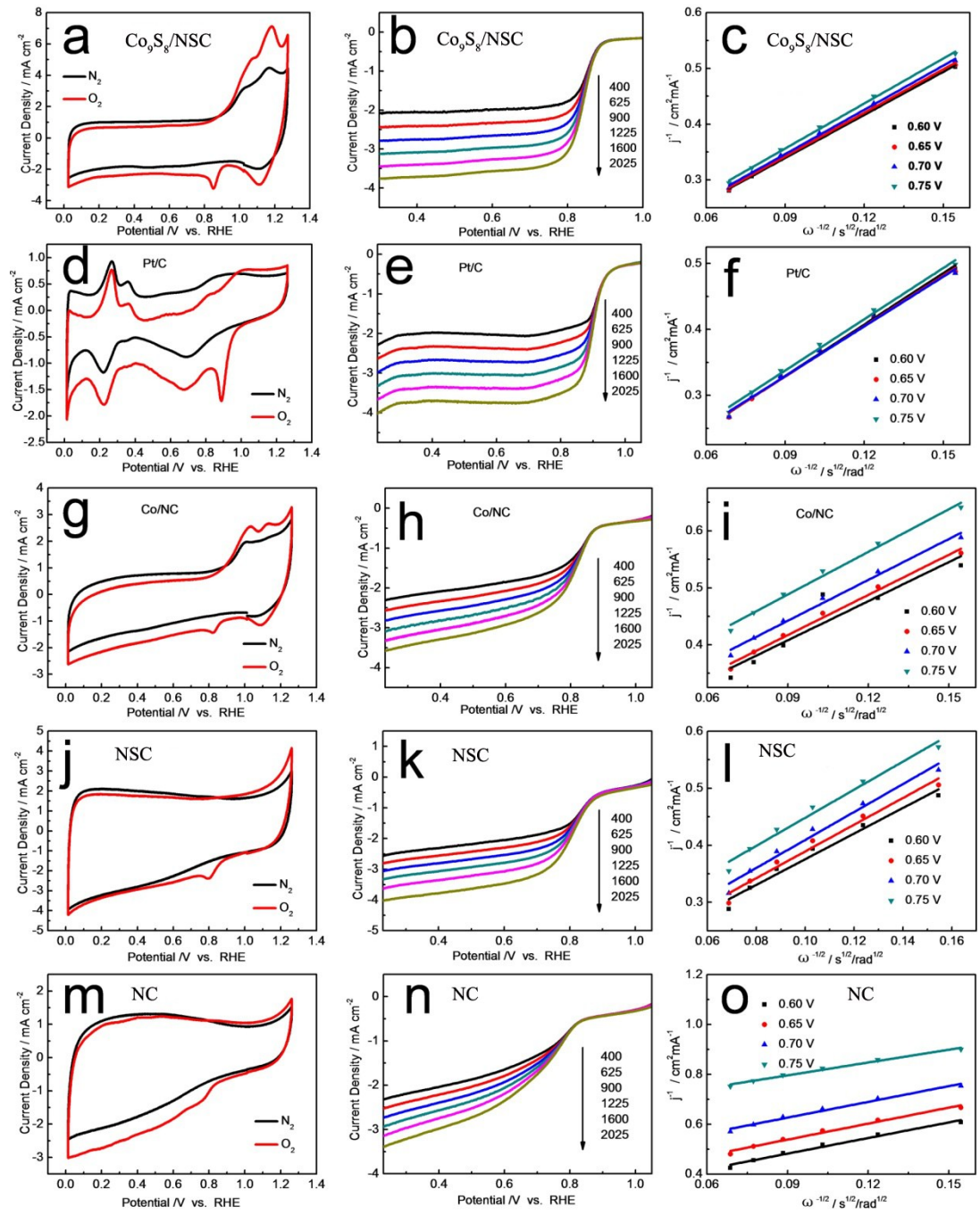


Figure S10. (a, d, g, j, m) CV curves of different catalysts in O_2 -saturated (red line) and N_2 -saturated (black line) 1 M KOH solution. (b, e, h, k, n) LSVs curves of different catalysts for ORR at different rotating speeds. (c, f, i, l, o) K-L plots of different catalysts at different potentials.

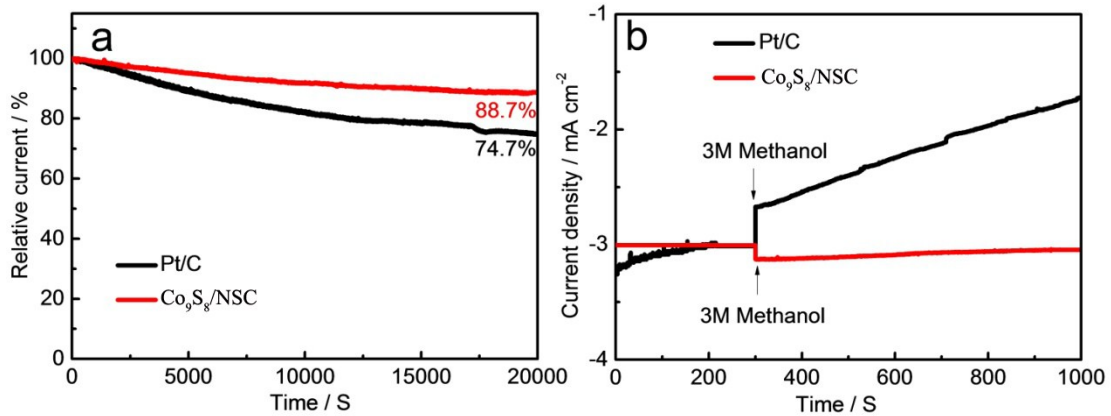


Figure S11. (a) Chronoamperometric curves of Co₉S₈/NSC nanofibers and Pt/C kept at 0.8 V vs. RHE. (b)

Chronoamperometric responses of Co₉S₈/NSC nanofibers and Pt/C at 0.8 V to the addition of 3.0 M methanol into

an O₂-saturated 1.0 M KOH solution with a rotation rate of 1600 rpm.

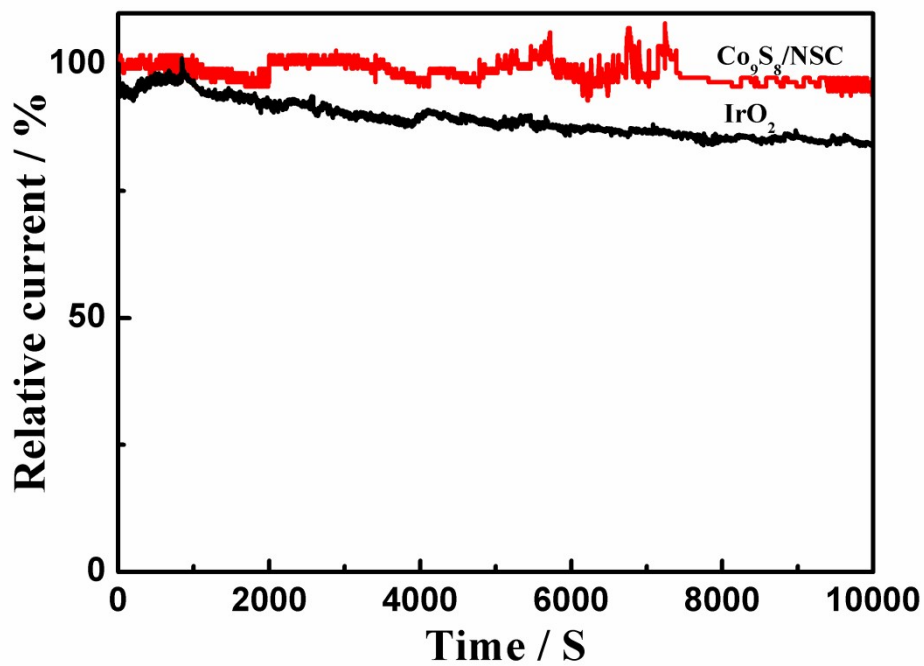


Figure S12. Chronoamperometric response at a constant potential of 1.7 V vs. RHE of Co₉S₈/NSC (red line) and

IrO₂ (black line) in 1 M KOH solution.

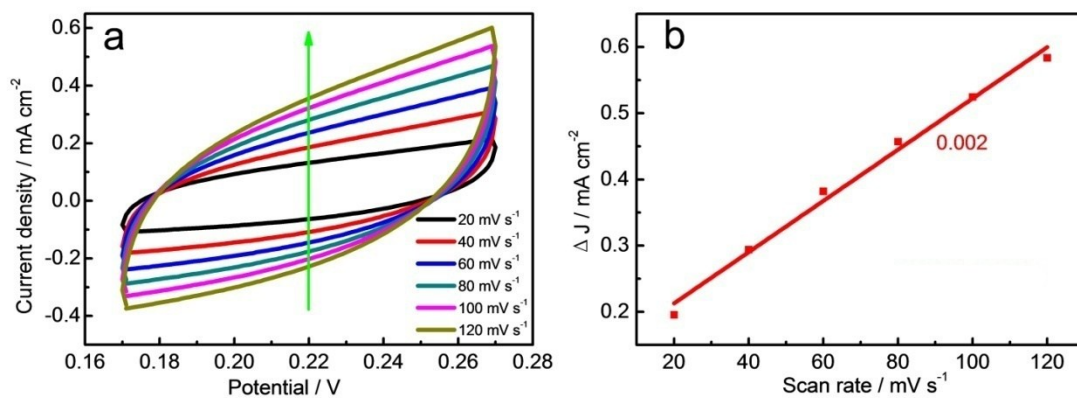


Figure S13. Typical cyclic voltammetry curves for (a) $\text{Co}_9\text{S}_8/\text{NSC}$ nanofibers and (b) Charge current density

differences (ΔJ) of $\text{Co}_9\text{S}_8/\text{NC}$ nanofibers electrodes plotted against scan rate. The linear slope, equivalent to twice

of the double-layer capacitance C_{dl} , was used to represent electrochemical active surface area (ECSA).

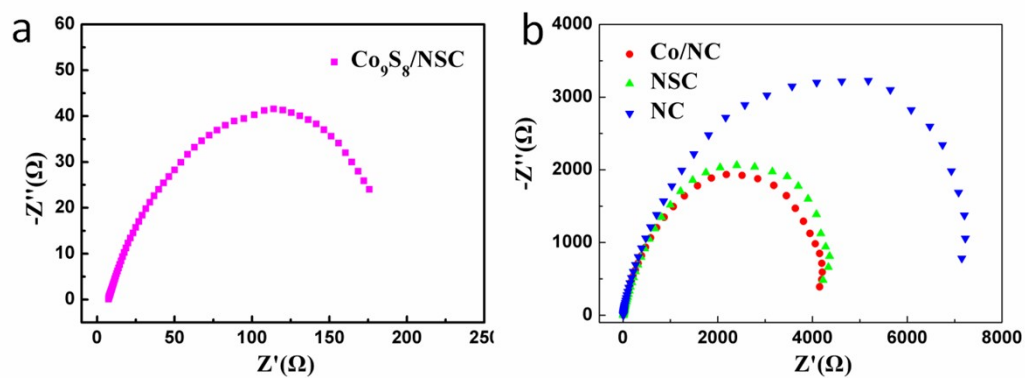


Figure S14. Nyquist plots of (a) $\text{Co}_9\text{S}_8/\text{NSC}$ nanofibers and (b) other catalysts at 0.55 V with a rotation rate of

1600 rpm.

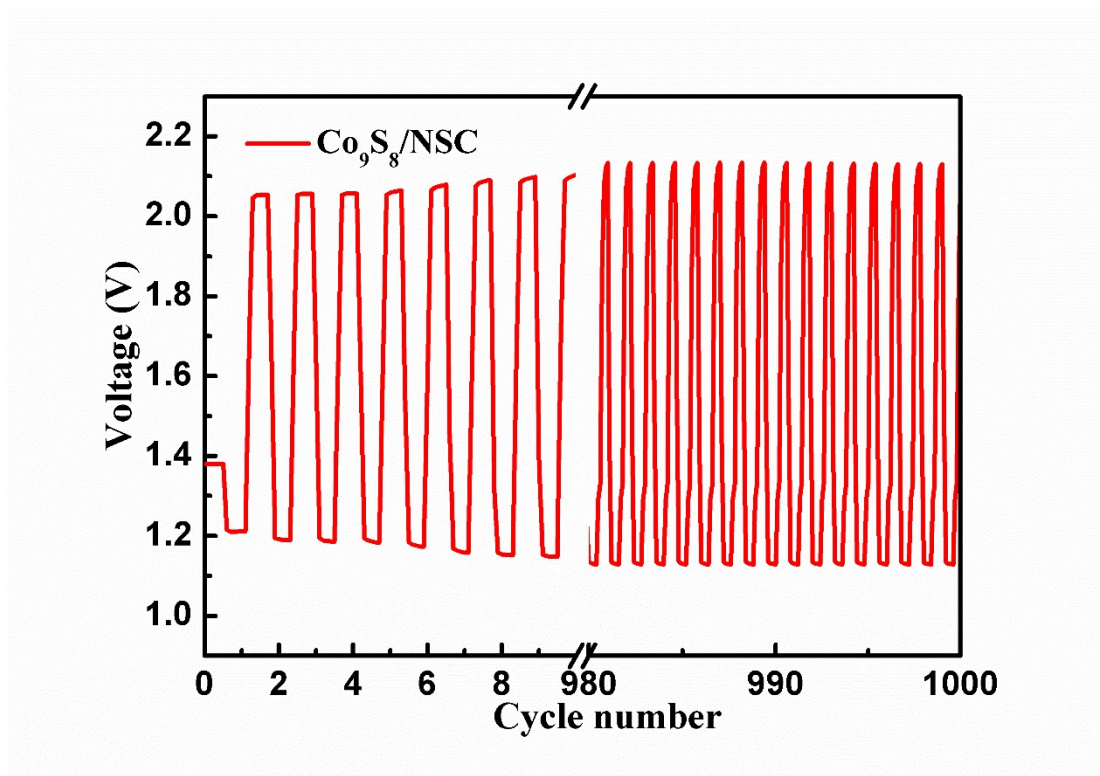


Figure S15. Galvanostatic discharge-charge cycling curves at 10 mA cm^{-2} of rechargeable Zn-air batteries with the $\text{Co}_9\text{S}_8/\text{NSC}$ nanofibers.

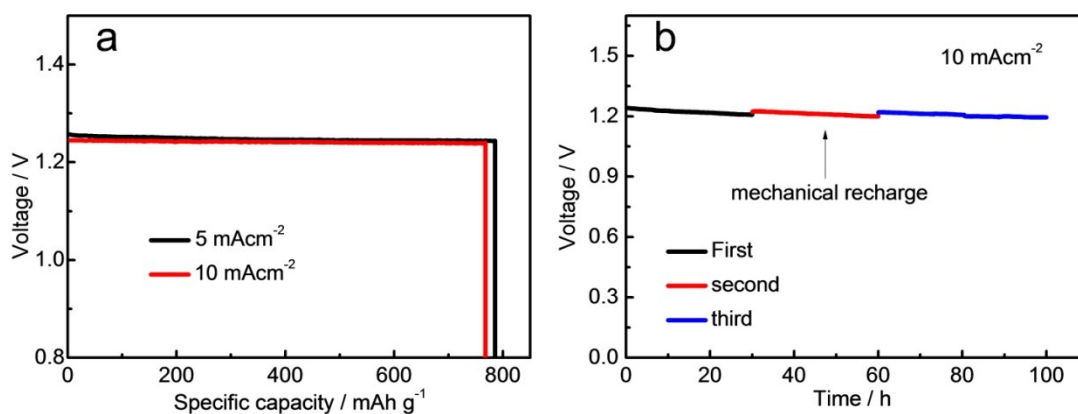


Figure S16. (a) Specific capacities for the Zn-air batteries using $\text{Co}_9\text{S}_8/\text{NSC}$ nanofibers as ORR catalysts, which were normalized with the mass of consumed Zn. (b) Long-term stability of the primary Zn-air battery with $\text{Co}_9\text{S}_8/\text{NSC}$ nanofibers cathode at 10 mA cm^{-2} . The battery was recharged by refilling the Zn anode and electrolyte.



Figure S17. Photograph of the battery with an open-circuit voltage of ~ 1.53 V.

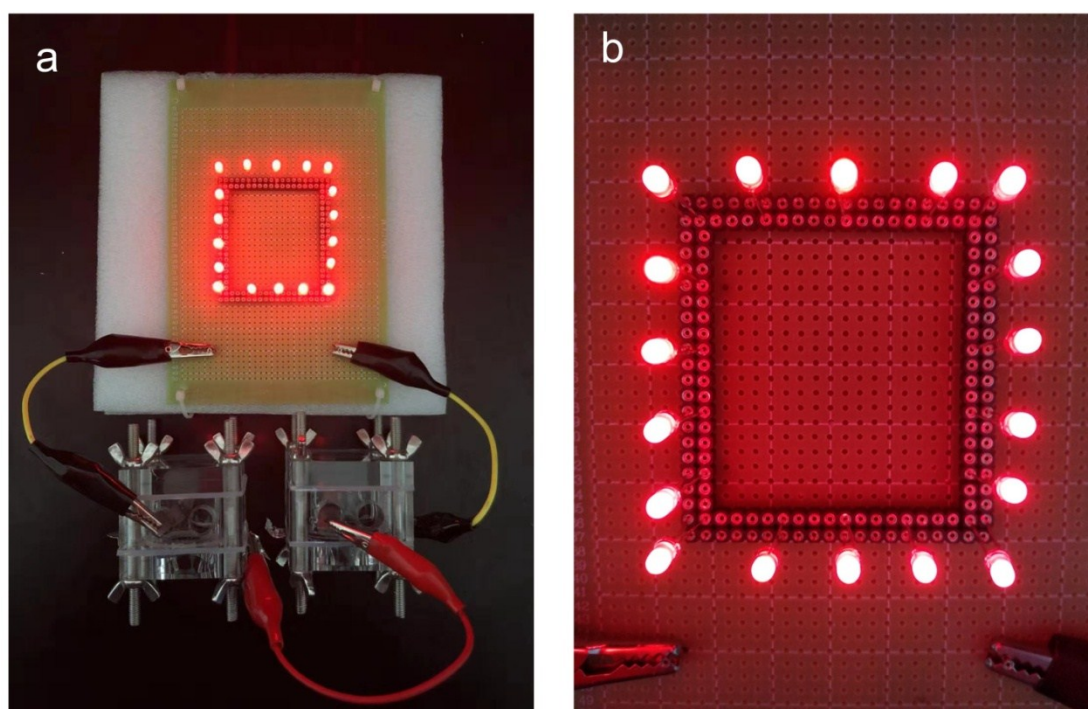


Figure S18. (a) (b) Photographs of 18 parallel red LED lamp beads driven by two Zn-air batteries with the $\text{Co}_9\text{S}_8/\text{NSC}$ nanofibers electrode connected in series.

Table S1. Elemental analysis of the Co₉S₈/NSC nanofibers, Co/NC nanofibers, NSC nanofibers, and NC nanofibers.

Sample	C (at.%)	N (at.%)	S (at.%)	Co (at.%)
Co ₉ S ₈ /NSC	67.55	2.95	8.16	1.61
Co/NC	74.53	4.23	-	1.41
NSC	73.14	4.03	10.07	-
NC	70.72	3.75	-	-

Table S2. Summary of the OER and ORR performances of the catalysts in this work and reported researches.

Catalyst	Electrolyte	ORR half-wave potential ($E_{1/2}$) (V vs. RHE)	OER potential @ 10 mA cm ⁻² ($E_{j=10}$) (V vs. RHE)	ΔE ($E_{j=10} - E_{1/2}$) (V)	Ref.
Co ₉ S ₈ /NSC	1 M KOH	0.84 V	1.56 V	0.72	This work
Co ₃ O ₄ NS/ZTC	1 M KOH	0.69 V	1.60 V	0.91	J. Mater. Chem. A, 2019, 7, 9988-9996
FeNi@HNC	1 M KOH	0.87 V	1.48 V	0.61	Sustainable Energy Fuels, 2019, 3, 136–141
Co ₉ S ₈ @NSCM	0.1 M KOH	0.81 V	1.60 V	0.79	Nanoscale, 2018, 10, 2649
CoO _{0.87} S _{0.13} /GN	0.1 M KOH	0.83 V	1.59 V	0.76	Adv. Mater. 2017, 29, 1702526
Ni ₃ Fe/N-C sheets	0.1 M KOH	0.86 V	1.62 V	0.84	Adv. Energy Mater. 2017, 7, 1601172.
Fe/N/C@BMZIF	0.1 M KOH	0.85 V	1.64 V	0.79	ACS Appl. Mater. Interfaces. 2017, 9, 5213-5221
Fe ₃ C/Co(Fe)O _x @N CNT	0.1 M KOH	0.86 V	1.58 V	0.72	ACS Appl. Mater. Interfaces. 2017, 9, 21216-21224
CoZn-NC-700	0.1 M KOH	0.84 V	1.62 V	0.78	Adv. Funct. Mater. 2017, 1700795.
Co ₄ N/CNW/CC	1 M KOH	0.8 V	1.54 V	0.74	J. Am. Chem. Soc. 2016, 138, 10226–10231
Co@Co ₃ O ₄ /NC-1	0.1 M KOH	0.79 V	1.65 V	0.86	Angew. Chem. Int. Ed. 2016, 55, 4087-4091
Carbon nanotube frameworks	0.1 M KOH	0.84 V	1.60 V	0.76	Nature Energy, 2016, 1, 15006